Electron Irradiation of Poly(3-hexylthiophene) Films

H. Ahn, D. W. Oblas, and J. E. Whitten*

The Department of Chemistry and Center for Advanced Materials, The University of Massachusetts Lowell, Lowell, Massachusetts 01854

Received December 24, 2003

ABSTRACT: The effects of low-energy electron irradiation on spin-coated films of regioregular poly(3-hexylthiophene) have been studied with fluorescence, mass spectrometry, and a variety of electron spectroscopies, including photoemission. Electron impact by 180 eV electrons causes a decrease in photoluminescence intensity, broadening of the thiophene ring valence electronic state features, and diminution in intensity of the peaks due to π electrons delocalized along the backbone. Electron bombardment also results in a decrease in the X-ray photoelectron spectroscopy sulfur-to-carbon ratio, but only minor shifts in the binding energies of the C 1s and S 2p peaks occur. Quadrupole mass spectrometry has been used to detect electron-stimulated desorption from the polymer films. Ionic desorption includes S^-, SH^-, S^+, and $C_xH_y^+$ species. Auger electron spectroscopy confirms removal of sulfur from the near-surface region by a 5 keV electron dose of 1.8×10^{18} electrons/cm^2, and electron energy loss spectroscopy suggests formation of a graphitic surface.

Introduction

Polythiophenes comprise an important class of organic semiconductors that are finding electroluminescent,[1−3] photovoltaic,[1,4] field-effect transistor,[5−7] corrosion protection,[8] and electromagnetic shielding[9] applications. Although electron beams are generally known to be destructive to organic and polymeric films,[10,11] there have been few studies of the effects of electron beam irradiation on conjugated polymers. Especially important is the electron dose required for significant decomposition and the nature of the resulting organic layer. These are critical issues with respect to the fabrication of organic electronic devices, since polymeric films may inadvertently be exposed to electrons during electron beam evaporation of metal electrodes or during surface analysis.[11,12] In one of the few published investigations, Bröms et al.[13] used photoluminescence and ultraviolet photoelectron spectroscopy (UPS) to study the effects of electron impact on poly(*p*-phenylenevinylene) films. The authors concluded that electron irradiation facilely leads to destruction of conjugation and loss of delocalization and causes a dramatic decrease in fluorescence intensity. The effects of low-energy electron bombardment of poly(3,4-ethylenedioxythiophene)-containing films have also recently been studied.[14] Interestingly, even electrons with energies as low as 3 eV were found to significantly decompose the organic layer.

A large body of literature[15,16] exists related to electron-stimulated desorption (ESD) and decomposition of monolayers, and to a lesser extent of multilayers, of adsorbates on metal surfaces. While there may be variations, electron-induced desorption and decomposition occur by the following general mechanism.[15−18] The kinetic energy of impinging electrons is converted to potential energy via electronic excitations of surface−adsorbate or intraadsorbate bonding states. Excitation to ionic or neutral repulsive states may lead to desorption as bonds break and the escaping neutral or ionic species recedes from the surface as potential energy is converted to kinetic energy. However, this recession is in competition with decay mechanisms, especially in the case of a nearby metal surface, which may redistribute the electronic energy and lead to recapture of the escaping ion or neutral particle.

In addition to being important for understanding the detrimental effects of electron irradiation, ESD has also been used to modify surfaces[19] and to determine the orientation of adsorbates.[20,21] It is surprising that so few studies have been carried out on polymeric systems. With respect to electron irradiation of nonconducting polymers, existing experiments include degradation studies of Teflon[22−24] and cross-linking studies of a perfluoroalkoxy resin[25] and low-density polyethylene.[26]

In the present work, we have investigated low-energy electron bombardment of thin films of regioregular poly(3-hexylthiophene), hereafter referred to as rr-P3HT. The chemical structure of P3HT is shown in Figure 1. This is one of the most commonly used polythiophenes for organic electronics, and the regioregular[27] form of the polymer permits the formation of spin-coated films with minimal conformational defects. X-ray and ultraviolet photoelectron spectroscopies (XPS and UPS), which are sensitive to the chemistry of the polymer surface, and fluorescence measurements have been used to determine the effects of electron irradiation on the electronic structure and chemistry of the polymer film. Quadrupole mass spectrometry has been used to directly detect species removed by electron impact. It is demonstrated that loss of photoluminescence intensity and destruction of delocalized electronic states are accompanied by desorption of sulfur-containing ions from the polymer surface. Extensive bombardment results in depletion of sulfur from the near-surface region. Neutral molecular hydrogen is also desorbed by electron impact, and electron energy loss spectroscopy suggests that electron irradiation leads to a graphitic surface. This represents the first study of the effects of electron irradiation of a polythiophene and the first report of the direct detection of sulfur by electron irradiation of an organic film.

Experimental Section

Sample Preparation. Films (350 Å) of rr-P3HT were prepared by spin-coating at 2000 rpm from a 0.2 wt % solution made by dissolving commercially available regioregular P3HT

10.1021/ma030589x CCC: $27.50 © 2004 American Chemical Society
Published on Web 04/01/2004

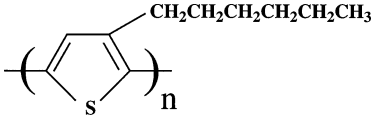

Poly[3-hexylthiophene]

Figure 1. Chemical structure of poly(3-hexylthiophene).

(Sigma Aldrich), having an average molecular weight of ca. 87 000, in chloroform. The films were spin-coated onto 1000 Å of gold that had been thermally deposited onto Si(111) wafers with areas of ca. 1 cm^2. Film thickness was measured by profilometry. The wafers were attached to stainless steel sample stubs via silver conductive adhesive (Electron Microscopy Sciences) that made electrical contact to the edges of the gold surface. Use of conductive substrates and relatively thin polymer films was necessary to avoid charging during the photoelectron spectroscopy measurements and to ensure that whatever voltage was placed on the sample stub (connected via an electrical feedthrough in the vacuum chamber) was the voltage on the sample surface. Charging of semiconducting conjugated polymer films is not significant for relatively thin films, and even films as thick as 2000 Å have been studied without problematic charging.[28]

Electron Spectroscopies. These were performed in a VG ESCALAB II instrument equipped with a concentric hemispherical electron energy analyzer, a Mg Kα X-ray source ($h\nu$ = 1253.6 eV), an He I ultraviolet lamp ($h\nu$ = 21.2 eV), and an electron gun. These radiation sources were used for X-ray and ultraviolet photoelectron spectroscopy (XPS and UPS) and Auger electron spectroscopy (AES) experiments, respectively. The X-ray and ultraviolet light sources were approximately at an angle of incidence of 45°, and photoelectrons were detected perpendicular to the sample plane. The samples were held at electrical ground during XPS and at −6.1 V for UPS. Binding energies for XPS and UPS measurements are reported with respect to the Fermi level of the metal substrate. For the XPS and UPS measurements, the electron energy analyzer was operated in fixed analyzer transmission (FAT) mode using pass energies of 20 and 2 eV, respectively. In the case of XPS and UPS, errors in the binding energies are estimated to be less than 0.10 eV based on calibration with clean gold samples. Electron energy loss spectroscopy was performed with the same electron gun used for AES. The vacuum in this instrument was in the low 10^{-9} mbar range, and all measurements were made at room temperature.

Electron Irradiation. The samples, at room temperature, were bombarded with electrons in several ways depending on the experiment. In most cases, a 0.1 mm diameter tungsten wire filament with coiled end sections was used, with the polymer/Au/Si(111) sample biased positive (45−180 V) relative to the filament. In this case, the sample could be turned to face the filament that was approximately 1.5 cm in front of the sample. This mode had the advantage of irradiating the entire surface of the sample with 45−180 eV electrons, which was desirable for photoelectron spectroscopy experiments that interrogate a fairly large area of the surface. Typically, electron emission currents of 0.55 μA were used. In the case of the Auger electron spectroscopy study, the same electron gun used for the Auger measurements was used for electron irradiation. The electron beam spot size in this case was approximately 1 mm^2, and the current was 38 nA.

Mass Spectrometry. For detecting neutral desorption, a quadrupole-based residual gas analyzer (RGA) was installed in the preparation chamber of the ESCALAB such that it was in line-of-sight of the P3HT/Au/Si(111) sample, which could be biased at different voltages with respect to ground. For ion detection, a quadrupole-based secondary ion mass spectrometer (VG SIMSLAB) was used. For these experiments, a primary ion beam was not employed, but a 500 eV flood gun was used for electron bombardment of the sample surface. Both positive and negative ions could be monitored by proper choice of electron optic voltages. The vacuum in this instrument was also in the low 10^{-9} mbar range.

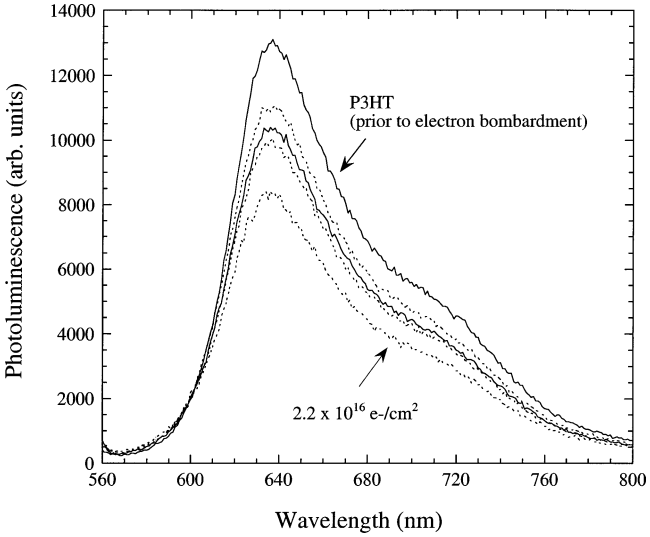

Figure 2. Photoluminescence spectra of a rr-P3HT film following 180 eV electron irradiation. The top spectrum is for the film prior to electron bombardment, and subsequent spectra (in order of decreasing photoluminescence intensity) correspond to 2.8×10^{15}, 5.6×10^{15}, 1.1×10^{16}, and 2.2×10^{16} electrons/cm^2. The excitation wavelength is 550 nm, and the excitation and emission slit widths are 1 mm.

Fluorescence Spectra. Photoluminescence spectra were acquired using a JY Horiba "Spex Fluorolog" instrument. The instrument was operated in reflection mode with a 22.5° angle between the excitation source and the detector.

Results and Discussion

Figure 2 shows the effects of 180 eV electron bombardment on the photoluminescence spectrum of a 350 Å spin-coated film of regioregular P3HT on a gold-coated Si(111) wafer. While the emission spectrum does not shift as a result of electron irradiation, its intensity decreases dramatically. These data demonstrate the deleterious effects that electron irradiation can have on the fluorescence intensity of conjugated polymer films. The decrease in photoluminescence is, as discussed below, the result of the destruction of thiophene ring and delocalized electronic states. It is also possible that defects act as photoluminescent quenching centers, as observed for poly(*p*-phenylenevinylene) films.[29]

The effects of 180 eV electron bombardment on the valence electronic structure of films of this polymer have been studied with He I UPS, and the results are shown in Figure 3. The peak at 4.0 eV is due to thiophene ring electronic states. Electron bombardment results in a broadening of this feature and a gradual diminution in intensity of the peaks near the Fermi level that are due to delocalized π electrons along the conjugated backbone.[30] Their disappearance indicates that electron bombardment results in destruction of delocalized electronic states. Similar conclusions were drawn from UPS investigations of electron irradiation of poly(*p*-phenylenevinylene) films.[13] The broadening of the 4.0 eV feature is consistent with a widening distribution of effective conjugation lengths (i.e., less homogeneous sample) as the P3HT is degraded.

Elemental analysis of the polymer surface (before electron irradiation) by Mg Kα XPS shows only carbon, sulfur, and traces of oxygen (estimated at 0.5 at. %) to be present; XPS does not detect hydrogen. No other elements, including gold from the substrate, were detectable. The inelastic mean free path of ejected

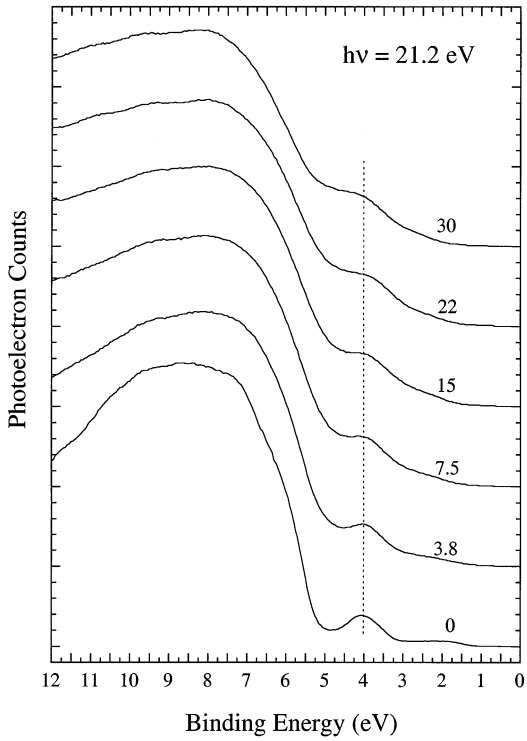

Figure 3. He I ultraviolet photoelectron spectroscopy of a 180 eV electron-irradiated rr-P3HT film. The number to the right of each spectrum corresponds to the cumulative electron dose in units of 10^{15} electrons/cm^2. The binding energy is relative to the Fermi level of the gold substrate.

photoelectrons (using Mg Kα radiation) is in the range 10−20 Å,[31] and gold photoelectrons cannot elastically escape through the 350 Å film. Using the areas of the C 1s and S 2p peaks and appropriate sensitivity factors,[32] the C/S atomic ratio is 12.2; similar analysis using the C 1s and S 2s peaks yields a ratio of 10.2. The theoretically expected ratio for P3HT is 10.0. These data indicate that, except for trace amounts of trapped oxygen, the films are contaminant-free.

Figures 4 and 5 show XPS spectra of the C 1s and S 2p regions, respectively, of rr-P3HT films as a function of electron dose. While it is not well-resolved, the shoulder to the high binding energy side of the main peak in Figure 5 is due to spin−orbit splitting of the S 2p peak. The S 2p spectrum (prior to electron bombardment) is consistent with a single chemical state of sulfur. Except for a small shift in the C 1s binding energy from 285.1 to 285.0 eV and an increase in the fwhm from 1.3 to 1.4 eV, extensive electron bombardment does not lead to significant changes. In the case of the S 2p spectrum, a shift occurs from a peak position of 164.3 eV (fwhm of 1.9 eV) for the unirradiated P3HT film to 164.0 eV (fwhm of 1.9 eV) following an electron dose of 3.0×10^{16} electrons/cm^2. These results thus demonstrate that electron-induced decomposition of the polymer by 180 eV electrons does not result in marked changes in the XPS spectra.

To further investigate the effects of electron irradiation on rr-P3HT films, we have used mass spectrometry to detect species desorbed by impinging electrons. Figures 6 and 7 display positive and negative ion desorption data, respectively, with the spectra obtained using the charge neutralization electron flood gun, collection optics, and quadrupole mass spectrometer of the secondary ion mass spectrometer.

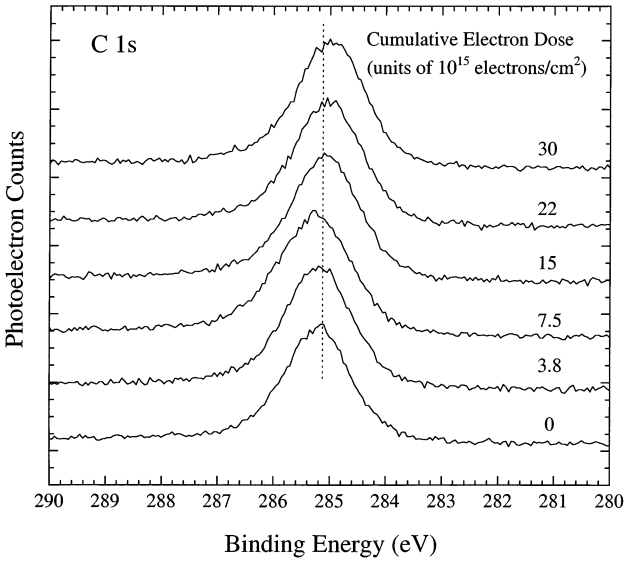

Figure 4. Mg Kα XPS of the C 1s region of a rr-P3HT film before and after 180 eV electron irradiation. The cumulative electron dose is included to the right of each spectrum. The binding energy is relative to the Fermi level of the gold substrate.

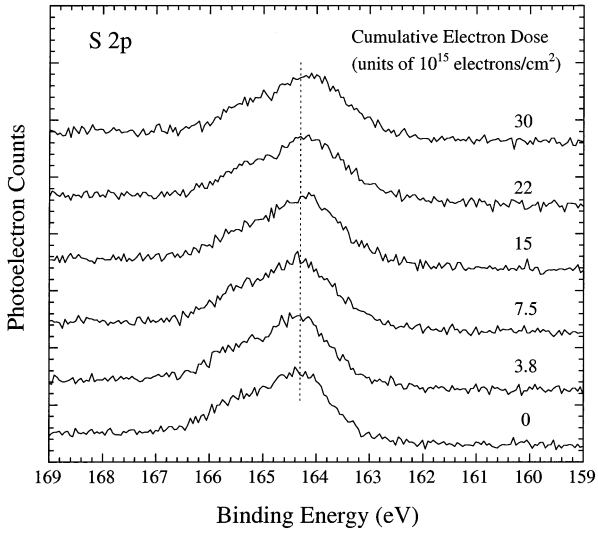

Figure 5. Mg Kα XPS of the S 2p region of a rr-P3HT film before and after 180 eV electron irradiation. The cumulative electron dose is included to the right of each spectrum. The binding energy is relative to the Fermi level of the gold substrate.

In the case of the positive ions (Figure 6), major detected species include CH_4^+, $C_2H_4^+$, $C_2H_3^+$, $C_2H_2^+$, S^+, and possibly $C_3H_8^+$, with the latter accounting for the $m/z = 44$ peak. It is also possible that this peak is due to CO_2^+. Confirmation that the $m/z = 32$ peak is due to sulfur is provided by detection of the $m/z = 33$ and 34 isotopes. However, their theoretical relative abundances are only 0.76 and 4.2%, respectively, compared to the $m/z = 32$ isotope.[33] That these peaks are more intense than theoretically expected, and that $m/z = 35$ is present, indicate that SH^+ is also desorbed by electron impact. The $m/z = 19$ peak is most likely due to F^+ originating from the periphery of the sample, which was coated with silver paint (see next paragraph).

The corresponding negative ion desorption spectrum is shown in Figure 7. Mainly sulfur-containing ions are detected from the P3HT film. These include peaks from the different isotopes of S^- and SH^-. The large F^- peak

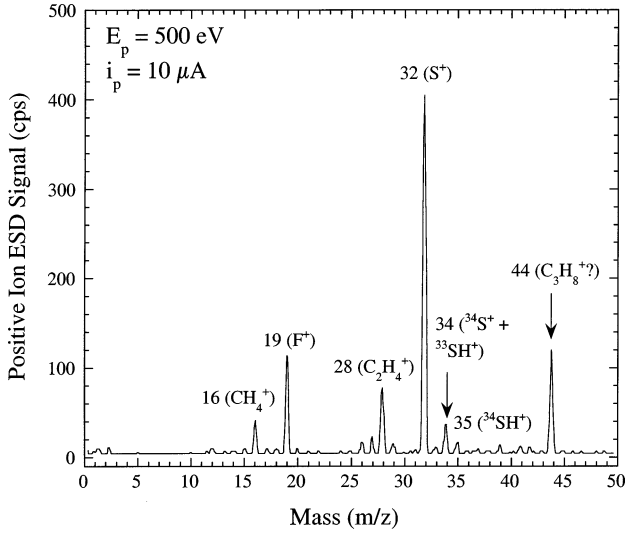

Figure 6. Mass spectrometry of positive ions desorbed from a rr-P3HT film by 500 eV electron irradiation. The F^+ signal originates from silver paint used on the edges of the sample.

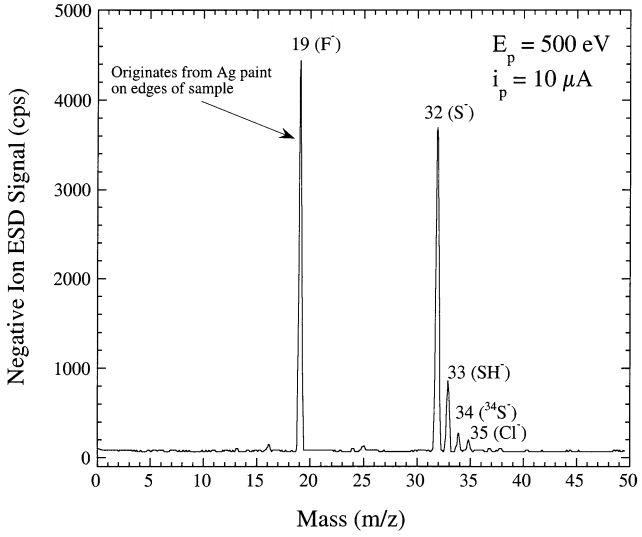

Figure 7. Mass spectrometry of negative ions desorbed from a rr-P3HT film by 500 eV electron irradiation. The F^- signal originates from silver paint used on the edges of the sample.

is due to silver paint used to electrically ground the sample around its edges. Fluorine is a component of the silver conductive adhesive used for these experiments, as indicated by XPS of a silver paint-coated sample stub. A control experiment in which the rr-P3HT/Au/Si sample was attached to a sample stub with metal clips instead of silver paint adhesive confirmed the origin of the F^+ and F^- signals to be the silver paint. The origin of the Cl^- is unknown; it may be due to small amounts of impurities in the polymer film that are not detectable by XPS.

It is important to note that, as in the case of ion desorption from sputtering experiments (i.e., SIMS), the probability of detection of a particular ionic species depends on several factors, including the stability of the ion and how readily it can escape from the surface without being recaptured or neutralized. Electronegative elements such as F and S are expected to form very stable negative ions. Furthermore, lighter masses will, in general, have higher escape cross sections due to their higher velocities (assuming the same or similar kinetic energies). Both of these factors favor F^- detection over

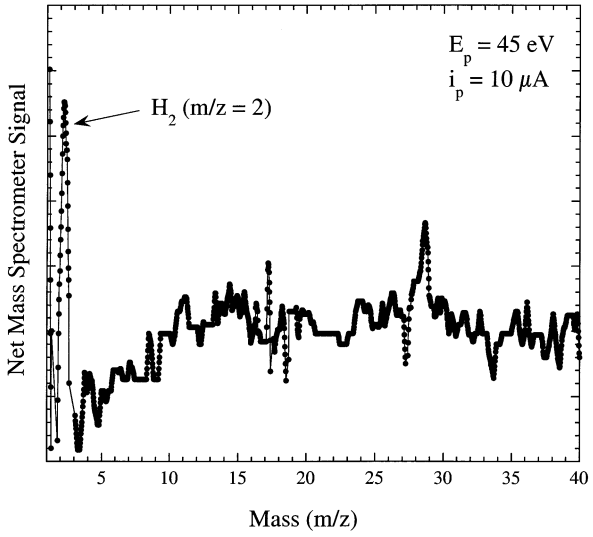

Figure 8. Mass spectrometry of neutral desorption from a rr-P3HT film by 45 eV electron irradiation. The small signals at $m/z = 18$ and 28 are likely artifacts of the background subtraction, as discussed in the text.

S^-. These account for the large F^- signal in Figure 7, even though the amount of fluorine in the silver paint is very small and the paint is only along the edges and occupying a small total area of the surface. Madey and colleagues have carried out various ESD studies on fluorine-containing small molecules, including SF_6 adsorbed on Ru(0001).[34,35] Both F^+ and F^- ions have been detected in these studies, and their angular distributions have been measured. The detection of these ions demonstrates their stability with respect to electron-induced desorption. While the authors did not apparently observe significant S^- desorption, S^+ was detected from SF_6 multilayers.[35] It must be recognized that ESD from a monolayer or thin multilayer adsorbate on a metal surface differs from that of a polymer film. A semiconducting polymer is not expected to be as efficient at quenching electronic excitations or recapturing desorbed ions as a metal surface.

It is surprising that so little H^+ and H^- signal is detected in the spectra of Figures 6 and 7. These are ordinarily the dominant ion signals observed from ESD of hydrocarbon films.[10,36] While Figure 6 does indicate a small amount of H^+, the intensities of these lower masses (in both Figures 6 and 7) are believed to be unreliable due to the fact that the transfer optics of the SIMSLAB were "tuned up" on the S^+ and S^- signals. Thus, it is possible that significantly greater H^+ (and possibly H^-) is desorbed than indicated in Figures 6 and 7.

Figure 8 shows neutral desorption from a 350 Å P3HT/Au/Si(111) sample, with the data obtained using the quadrupole-based residual gas analyzer in the ESCA preparation chamber, as described earlier. In this setup, an electrically grounded filament that irradiated the polymer surface with low-energy electrons resided between the sample and the RGA. The data were obtained by subtracting a background spectrum, measured with the filament at its operating temperature but with the sample at electrical ground, from an identical run measured with the sample at +45 V. This resulted in a spectrum representing the net signal due to 45 eV electron bombardment. As shown in Figure 8, neutral desorption consists mainly of molecular hydrogen. The small signals at $m/z = 18$ and 28 are likely

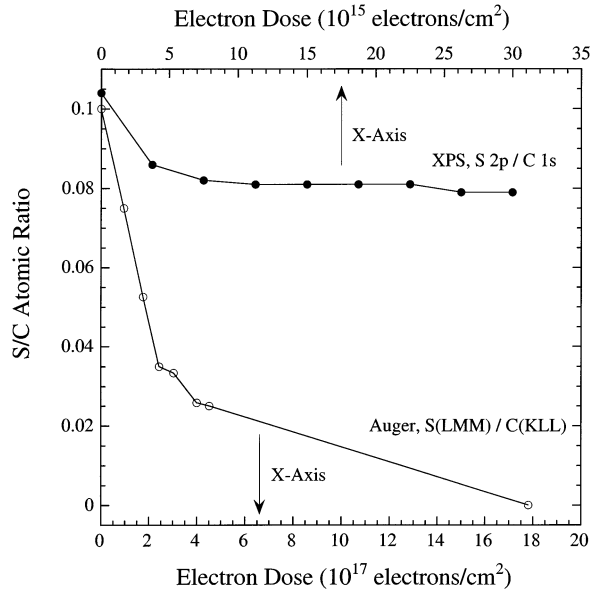

Figure 9. XPS and Auger electron spectroscopy sulfur-to-carbon atomic ratios vs electron dose for irradiation of rr-P3HT films. For the XPS study, 180 eV electrons were used for desorption/decomposition. For the Auger experiments, 5000 eV electrons were employed. The *x*-axis on the top of the graph is for the XPS study, while the bottom one is for the Auger experiments. The XPS ratios were obtained by integrating the S 2p and C 1s peaks, and the Auger ratios were obtained by measuring the peak-to-peak intensities of the C(KLL) and S(LMM) differentiated Auger peaks.

artifacts of the background subtraction (due to differences in the background levels of H_2O and CO) or possibly the result of electron-stimulated desorption from the sample stub. Neutral H_2 desorption was also detected by Whitten and Gomer[36] in ESD experiments on multilayer benzene condensed on a tungsten surface. In that work, and in the present study, molecular hydrogen must certainly result from the combination of neutral or ionic hydrogen atoms originating from C−H bond cleavage.

While no neutral sulfur-containing species are detected, extensive electron bombardment results in depletion of sulfur from the surface of the polymer film. This is demonstrated in Figure 9, which displays the results of an Auger electron spectroscopy study using 5 keV electrons. The data were obtained by measuring the peak-to-peak intensities of the S(LMM) and C(KLL) differentiated peaks and correcting for their sensitivity factors, which were taken as 0.70 and 0.14, respectively.[37] By a dose of 1.8×10^{18} electrons/cm^2, the S(LMM)/C(KLL) ratio has been reduced to essentially zero. Figure 9 also displays Mg Kα XPS results, obtained in a separate experiment on a different P3HT film, of the S 2p/C 1s ratio. In contrast to the 5 keV Auger data, the sulfur signal does not decrease to zero; only a ca. 20% decrease in signal is observed. Furthermore, the electron dose required to decay to half of the final S/C value is 2.6×10^{15} electrons/cm^2, which is much lower than the corresponding Auger experiment.

The apparent discrepancies between the XPS and Auger data are partially explained by the differences in mean free paths of electrons of different kinetic energies. The inelastic mean free path (IMFP) of electrons in poly(3-octylthiophene) films has recently been measured,[38] but the effects of electron irradiation were not investigated. No data were reported for P3HT; however, the results would be expected to be very similar. The following empirical expression was found to model the IMFP as a function of electron kinetic energy in the range 200−5000 eV:

$$\lambda = kE^p \qquad (1)$$

where λ is the mean free path, E is the electron energy, and k and p are fitting parameters. For poly(3-octylthiophene), k and p are 0.06144 and 0.9278, respectively.[38] Because the "universal" inelastic mean free path curve is monotonic and flat in the energy range 100−200 eV,[31] it is reasonable that this equation may be extended down to 150 eV with only minimal error.

The role of the electron IMFP is not as significant in the case of the impinging electrons as it is for the escaping electrons detected in the electron spectroscopy experiments. This is a result of the fact that the cross sections of the events leading to bond breaking and desorption do not depend strongly on electron energy, and even electrons that have lost energy in traversing through the organic layers can cause decomposition/desorption. In the case of the Auger experiment in Figure 9, 5 keV incident electrons were used. For this energy, the IMFP calculated from eq 1 is ca. 160 Å, while the IMFP of 180 eV electrons (as used for irradiation in the XPS experiment) is ca. 7.6 Å. Because the exciting electrons used in the Auger experiment penetrate deeper than the electrons used in the XPS experiment, they are distributed in a greater volume. Thus, a greater number per irradiated area are required to cause the same amount of decomposition detected from a small region near the surface. This accounts (at least partially) for the differences between the XPS and Auger curves of Figure 9.

For the S(LMM) and C(KLL) Auger peaks, the kinetic energies of the escaping electrons are 152 and 272 eV, respectively. These have relatively small IMFP values, estimated from eq 1 to be 6.5 and 11 Å, respectively. However, for the C 1s and S 2p XPS photoelectrons, the kinetic energies are 969 and 1090 eV, with inelastic mean free paths of 30−40 Å. Because the escaping XPS photoelectrons originate from a greater depth than penetrated by the 180 eV electrons used for irradiation, the sulfur signal never decays to zero.

Mass spectrometry has also been used to monitor the decay of the S^- signal as a function of 500 eV electron dose, as shown in Figure 10. The IMFP of the impinging electrons, in this experiment, is ca. 20 Å. Note, however, as discussed previously, that even these electrons will possess enough energy to decompose/desorb deeper in the sample than indicated by the IMFP. By a dose of 3×10^{15} electrons/cm^2, the S^- signal has decayed to about half of its initial value, falling off approximately in the same fashion as the 180 eV electron irradiation data in Figure 9. However, in the case of Figure 10, the S^- signal decays almost to zero, in contrast to the XPS study. As discussed earlier, this is a result of the XPS photoelectrons escaping from deeper in the sample than the depth penetrated by the impinging electron beam used for decomposition/desorption. For the S^- mass spectrometry study, of course, desorption and decomposition occur simultaneously, and removal of sulfur from the depth probed by the experiment is expected. Using the initial data of Figure 10 (up to a dose of 4×10^{15} electrons/cm^2) and assuming that the decay of the desorption signal follows first-order kinetics, the S^- desorption cross section is calculated to be 2.5×10^{-18} cm^2.

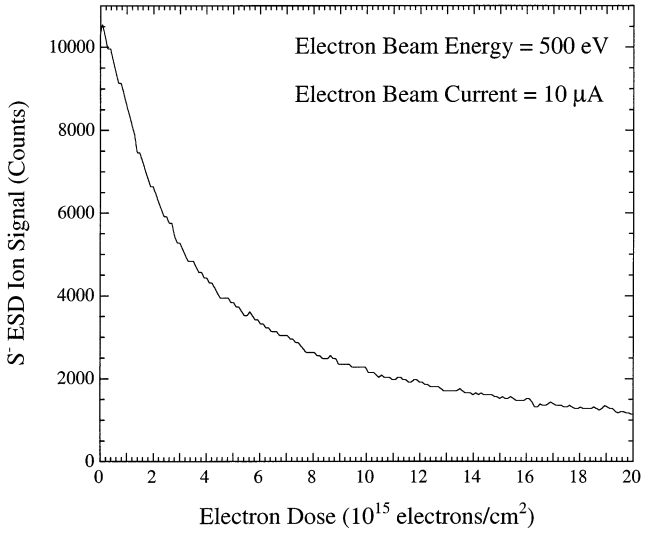

Figure 10. Decay of the S^- ESD ion signal vs 500 eV electron dose for a rr-P3HT film. These data were acquired by monitoring the S^- signal (as shown in Figure 7) during electron irradiation.

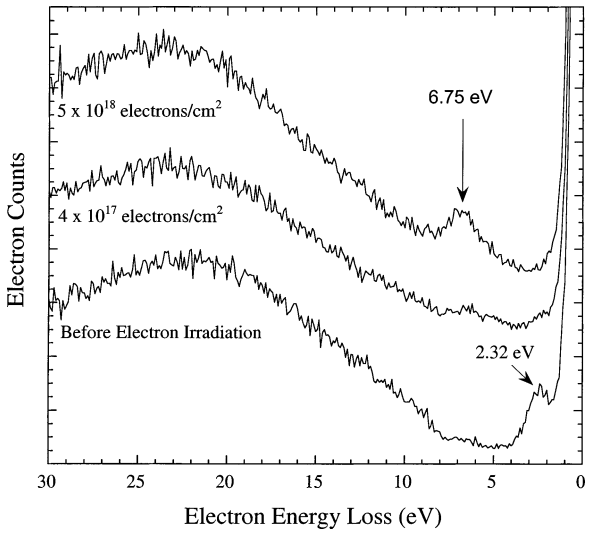

Figure 11. Electron energy loss spectroscopy of a rr-P3HT film before and after irradiation with 5000 eV electrons at doses of 4×10^{17} and 5×10^{18} electrons/cm^2. For the ELS measurements, an electron beam energy of approximately 1000 eV and current of 1.4 nA were used.

Without detailed studies of the kinetic energy distributions of the ejected ions and measurements of the thresholds of the energies of electrons needed to decompose/dissociate the rr-P3HT, it is difficult to discern the operative desorption mechanisms. Possibilities include dissociative electron attachment, dipolar dissociation, and core hole production that leads to desorption. Future experiments are needed to determine which of these are most important for semiconducting polymer films.

What is the nature of the surface of the resulting film? While the C 1s and S 2p XPS peaks do not exhibit significant peak shifts following 180 eV electron irradiation, partly due to the fact that the photoelectrons originate from deep in the sample, electron energy loss spectroscopy suggests that the resulting surface is graphitic. Figure 11 shows electron energy loss spectra of a virgin rr-P3HT film (prior to 5 keV electron bombardment) and spectra following electron doses of 4×10^{17} and 5×10^{18} electrons/cm^2. Prior to electron bombardment, a loss feature at ca. 2.3 eV is present which corresponds to the $\pi-\pi^*$ transition in the rr-P3HT film, as indicated by its agreement with the optical excitation maximum at 520−530 nm.[39] Agreement between optical absorption and electron energy loss spectroscopic observations for conjugated polymers has previously been observed.[40] This peak is replaced by one at 6.75 eV following extensive electron irradiation. The appearance of this higher energy feature only occurs as the sulfur Auger signal disappears. Graphite has a reported π plasmon (i.e., collective electronic excitation) at ca. 7 eV.[41] The emergence of this low-energy feature following electron irradiation strongly suggests that the resulting surface of the rr-P3HT film is graphitic in character. This is a reasonable outcome of extensive electron bombardment since graphite is the most thermodynamically stable form of carbon. It should also be noted that the region bombarded by electrons can be visually detected on the sample upon its removal from the vacuum chamber. Instead of the red color characteristic of the rr-P3HT film, the irradiated region appears "bleached out" and colorless. The lack of a black appearance, as might be expected for graphite, may be due to the thinness of the graphitic layer.

Holdcroft and colleagues[42−45] have studied the photochemistry of solutions and films of P3HT. When irradiated by UV−vis light, P3HT dissolved in organic solvents undergoes photobleaching, chain scission, and cross-linking; this process is most efficient in the presence of oxygen and in solvents that promote free-radical reactions.[42,43] In the case of thin films, cross-linking and insolubilization are found to occur.[44] These authors also have demonstrated direct-write laser microlithography by dissolution of unexposed P3HT regions.[45] In the present study, electron irradiation leads to the complete disappearance of sulfur from the near-surface region, and this apparently occurs with concomitant cross-linking that eventually leads to graphite formation as C−H bonds break and H_2 is desorbed. In addition to illustrating the care that must be taken to avoid electron exposure of conjugated polymers, this work shows that possibilities may exist for using electron beams to lithographically form conducting graphitic patterns on semiconducting conjugated polymer films.

Conclusions

These studies demonstrate that low-energy electron irradiation (180−5000 eV) of rr-P3HT films results in a decrease in photoluminescence intensity due to destruction of thiophene ring and delocalized electronic states. Neutral molecular hydrogen and a variety of molecular ions are desorbed by electron impact. These include sulfur-containing anions and C_xH_y cations. Extensive electron bombardment results in complete removal of sulfur from the near-surface region. Electron energy loss spectroscopy indicates that a graphitic surface is realized only after loss of conjugation and upon removal of sulfur from the near-surface region. This work clearly shows that inadvertent exposure of rr-P3HT films to even small doses of electrons results in changes in the electronic properties, changes in stoichiometry, and formation of defects in the near-surface region. Extensive irradiation leads to formation of a graphitic surface.

Acknowledgment. This work is based on research supported by the National Science Foundation under Grant DMR-008960.

References and Notes

(1) Granström, M.; Harrison, M. G.; Friend, R. H. In *Handbook of Oligo- and Polythiophenes*; Fichou, D., Ed.; Wiley-VCH: Weinheim, 1999; pp 405−458.
(2) Endo, T.; Rikukawa, M.; Sanui, K. *Synth. Met.* **2001**, *119*, 191−192.
(3) Bao, Z.; Rogers, J. A.; Dodabalapur, A.; Lovinger, A. J.; Katz, H. E.; Raju, V. R.; Peng, Z.; Galvin, M. E. *Opt. Mater.* **1999**, *12*, 177−182.
(4) Too, C. O.; Wallace, G. G.; Burrell, A. K.; Collis, G. E.; Officer, D. L.; Boge, E. W.; Brodie, S. G.; Evans, E. J. *Synth. Met.* **2001**, *123*, 53−60.
(5) Katz, H. E.; Dodabalapur, A.; Bao, Z. In *Handbook of Oligo- and Polythiophenes*; Fichou, D., Ed.; Wiley-VCH: Weinheim, 1999; pp 459−489.
(6) Garnier, F. *Chem. Phys.* **1998**, *227*, 253−262.
(7) Babel, A.; Jenekhe, S. A. *Macromolecules* **2003**, *36*, 7759−7764.
(8) Yu, Y.-J.; Kim, J.-G.; Boo, J.-H. *J. Mater. Sci., Lett.* **2002**, *21*, 951−953.
(9) Kossmehl, G.; Engelman, G. In *Handbook of Oligo- and Polythiophenes;* Fichou, D., Ed.; Wiley-VCH: Weinheim, 1999; pp 491−524.
(10) Sanche, L. *Nucl. Instrum. Methods B* **2003**, *208*, 4−10.
(11) Gilmore, I. S.; Seah, M. P. *Appl. Surf. Sci.* **2002**, *187*, 89−100.
(12) Gardella, J. A., Jr.; Pireaux, J. J. *Anal. Chem.* **1990**, *62*, 645A−661A.
(13) Bröms, P.; Johansson, N.; Gymer, R. W.; Graham, S. C.; Friend, R. H.; Salaneck, W. R. *Adv. Mater.* **1999**, *11*, 826−832.
(14) Denier van der Gon, A. W.; Birgerson, J.; Fahlman, M.; Salaneck, W. R. *Org. Electron.* **2002**, *3*, 111−118.
(15) Madey, T. E. *Surf. Sci.* **1994**, *299*−*300*, 824−836.
(16) Ramsier, R. D.; Yates, J. T. *Surf. Sci. Rep.* **1991**, *12*, 243−378.
(17) Menzel, D.; Gomer, R. *J. Chem. Phys.* **1964**, *41*, 3311−3328.
(18) Redhead, P. A. *Can. J. Phys.* **1964**, *42*, 886−905.
(19) Avouris, P.; Bozso, F.; Walkup, R. E. *Phys. Rev. Lett.* **1986**, *57*, 1185−1188.
(20) Madey, T. E.; Benndorf, C.; Shinn, N. D. In *Desorption Induced by Electronic Transitions (DIET 2);* Springer-Verlag: Berlin, 1985; pp 104−115.
(21) Yates, J. T., Jr.; Alvey, M. D.; Kolasinski, K. W.; Dresser, M. J. *Nucl. Instrum. Methods B* **1987**, *B27*, 147−154.
(22) Chinaglia, D. L.; Hessel, R.; Oliveira, O. N. *Polym. Degrad. Stab.* **2001**, *74*, 97−101.
(23) Clark, D. T.; Brennan, W. J. *J. Electron. Spectrosc. Relat. Phenom.* **1986**, *41*, 399−410.
(24) Duraud, J. P.; Le Moel, A.; Le Gressus, C. *Radiat. Effects* **1986**, *98*, 151−157.
(25) Dargaville, T. R.; George, G. A.; Hill, D. J. T.; Scheler, U.; Whittaker, A. K. *Macromolecules* **2003**, *36*, 7138−7142.
(26) Al-Qaradawi, I. Y. *Radiat. Phys. Chem.* **2003**, *68*, 467−470.
(27) Chen, T.-A.; Wu, X.; Rieke, R. D. *J. Am. Chem. Soc.* **1995**, *117*, 233−244.
(28) Salaneck, W. R.; Stafström, S.; Brédas, J.-L. *Conjugated Polymer Surfaces and Interfaces*; Cambridge University Press: Cambridge, 1996; p 43.
(29) Yan, M.; Rothberg, L. J.; Papadimitrakopoulos, F.; Galvin, M. E.; Miller, T. M. *Phys. Rev. Lett.* **1994**, *73*, 744−747.
(30) Dannetun, P.; Boman, M.; Stafström, S.; Salaneck, W. R.; Lazzaroni, R.; Fredriksson, C.; Brédas, J. L.; Zamboni, R.; Taliani, C. *J. Chem. Phys.* **1993**, *99*, 664−672.
(31) Feldman, L. C.; Mayer, J. W. *Fundamentals of Surface and Thin Film Analysis*; Elsevier: New York, 1986; p 129.
(32) Scofield, J. H. *J. Electron Spectrosc.* **1976**, *8*, 129−137.
(33) Feldman, L. C.; Mayer, J. W. *Fundamentals of Surface and Thin Film Analysis*; Elsevier: New York, 1986; p 334.
(34) Faradzhev, N. S.; Kusmierek, D. O.; Yakshinskiy, B. V.; Solovev, S. M.; Madey, T. E. *Surf. Sci.* **2003**, *528*, 20−26.
(35) Faradzhev, N. S.; Kusmierek, D. O.; Yakshinskiy, B. V.; Madey, T. E. *Low Temp. Phys.* **2003**, *29*, 215−222.
(36) Whitten, J. E.; Gomer, R. *Surf. Sci.* **1996**, *347*, 280−288.
(37) Davis, L. E.; MacDonald, N. C.; Palmberg, P. W.; Riach, G. E.; Weber, R. E. *Handbook of Auger Electron Spectroscopy*, 2nd ed.; Perkin-Elmer Corp.: Eden Prairie, MN, 1978; p 14.
(38) Lesiak, B.; Kosinski, A.; Jablonski, A.; Kövér, L.; Tóth, J.; Varga, D.; Cserny, I.; Zagorska, M.; Kulszewicz-Bajer, I.; Gergely, G. *Appl. Surf. Sci.* **2001**, *174*, 70−85.
(39) Ahn, H.; Whitten, J. E. *J. Phys. Chem. B* **2002**, *106*, 11404−11405.
(40) Hong, S. Y.; Marynick, D. S. *J. Chem. Phys.* **1992**, *96*, 5497−5504.
(41) Huang, C. S.; Lin, M. F.; Chuu, D. S. *Solid State Commun.* **1997**, *103*, 603−606.
(42) Holdcroft, S. *Macromolecules* **1991**, *24*, 4834−4838.
(43) Abdou, M. S.; Holdcroft, S. *Macromolecules* **1993**, *26*, 2954−2962.
(44) Abdou, M. S. A.; Diaz-Guijada, G. A.; Arroyo, M. I.; Holdcroft, S. *Chem. Mater.* **1991**, *3*, 1003−1006.
(45) Abdou, M. S. A.; Zi, W. X.; Leung, A. M.; Holdcroft, S. *Synth. Met.* **1992**, *52*, 159−170.

MA030589X